Inorganic Chemistry

pubs.acs.org/IC Communication

Synthesis of Antiperovskite Solid Electrolytes: Comparing Li_3SI, Na_3SI, and Ag_3SI

Liang Yin, Megan Murphy, Kwangnam Kim, Linhua Hu, Jordi Cabana, Donald J. Siegel, and Saul H. Lapidus*

Cite This: *Inorg. Chem.* 2020, 59, 11244−11247 Read Online

ACCESS | Metrics & More | Article Recommendations | Supporting Information

ABSTRACT: Prior calculations have predicted that chalcohalide antiperovskites may exhibit enhanced ionic mobility compared to oxyhalide antiperovskites as solid-state electrolytes. Here, the synthesis of Ag-, Li-, and Na-based chalcohalide antiperovskites is investigated using first-principles calculations and *in situ* synchrotron X-ray diffraction. These techniques demonstrate that the formation of Ag_3SI is facilitated by the adoption of a common body centered cubic packing of S^{2-} and I^- in the reactants and products at elevated temperatures, with additional stabilization achieved by the formation of a solid solution of the anions. The absence of these two features appears to hinder the formation of the analogous Li and Na antiperovskites.

The development of all-solid-state batteries has attracted increasing attention in recent years. The adoption of solid-state electrolytes (SSEs) in place of conventional organic liquid electrolytes is projected to enable the use of high voltage cathode materials and high capacity metallic anodes. Solid electrolytes also greatly enhance battery safety.[1,2] The advantages of solid-state rechargeable batteries have motivated the search for inorganic solid-state ionic conductors. Several categories of SSEs with ionic conductivity comparable to that of liquids have been identified including glass-ceramic-type lithium sulfides, NASICON-type phosphates, garnet-type $Li_7La_3Zr_2O_{12}$, and antiperovskites (A_3OX, with A = Li, Na; X = Cl, Br) etc.[3] However, the practical application of SSEs still remains challenging.[4,5] Some of these challenges can be traced to the need for higher ionic conductivity (>10^{-2} S cm^{-1}), better chemical stability against electrodes, a wide electrochemical window, and mechanical resilience.[6−8]

The antiperovskite (AP) family has been known as ionic conductors for more than half a century.[9,10] In recent years, Li-based APs, such as Li_3OCl, Li_3OBr, and $Li_3OCl_{0.5}Br_{0.5}$, have attracted considerable attention as potential candidates for solid-state batteries because of their good electrochemical stability against Li metal, high ionic conductivity (above 10^{-3} S cm^{-1} at room temperature), low activation enthalpy, negligible electronic conductivity, good cyclability, moderate weight, and low cost.[11] Na-based antiperovskites have also been reported as potential solid electrolytes for use in sodium batteries.[12,13] Nevertheless, additional improvements to the performance of antiperovskite SSEs are desirable.

In 2019, a correlation was reported between the ion migration barriers in antiperovskites and their degree of lattice distortion, which could be tuned through substitutions on the anion sublattice: for example, substituting O^{2-} by S^{2-} or Cl^-/Br^- by I^-.[14] In this work, Na_3SI and Li_3SI were predicted as new (or "hypothetical") antiperovskites with the potential to exhibit higher mobility for Na^+ and Li^+, respectively. Nevertheless, the larger distortions of the antiperovskite lattice resulting from such substitutions were predicted to come at a cost to stability:[14] Na_3SI and Li_3SI are predicted to be unstable relative to metal chalcogenide and halide reagents at low temperature, but entropic contributions are expected to stabilize them upon heating (Figure 1).[15] Similar to Li_3OBr,[16] these materials could potentially be realized as kinetically stabilized phases at ambient temperature, following synthesis at, and quenching from, the higher temperatures at which they are stable.

Unfortunately, preliminary attempts to synthesize Na_3SI and Li_3SI have not been successful thus far. In contrast, the Ag_3SI antiperovskite is a well-known fast ionic conductor.[17−20] At least four different polymorphs of Ag_3SI, namely, α, α^*, β, and γ, have been observed at different temperatures.[9,10,18,21] These polymorphs differ in their ordering of S^{2-}/I^- and the location of Ag^+ within interspaces between anions. The S^{2-}/I^- disordered α-Ag_3SI is a superionic phase (ionic conductivity: ∼1.5 S cm^{-1} above 520 K). α^*-Ag_3SI, which differs from α-Ag_3SI in the positions of the Ag ions, has an ionic conductivity of ∼0.13 S cm^{-1} at ambient temperature. In contrast, the ionic conductivity of S^{2-}/I^-ordered β-Ag_3SI is approximately two orders of magnitude lower than that of α^*-Ag_3SI.[22]

Similar to Na_3SI and Li_3SI, Ag_3SI is predicted by DFT calculations to be unstable with respect to AgI and Ag_2S at low temperatures as shown in Figures 1 and S1. However, their stabilities increase as temperature rises. Given the similar free-energy behavior across these antiperovskites, the difference in our ability to synthesize them is surprising. If the formation mechanism associated with the synthesis of Ag_3SI could be

Received: June 9, 2020
Published: July 28, 2020

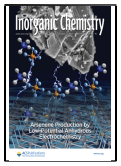

https://dx.doi.org/10.1021/acs.inorgchem.0c01705
Inorg. Chem. 2020, 59, 11244−11247

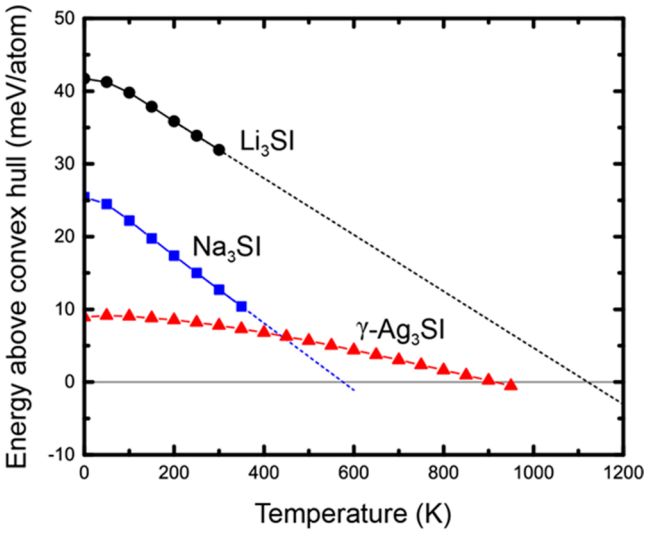

Figure 1. Energy above the convex hull, ΔG (given by $\Delta G = G_{A_3SI} - (G_{A_2S} + G_{AI})$, A = Li, Na, and Ag) as a function of temperature. (A description of the computational methodology can be found in the Supporting Information.) The simulation results for Li_3SI and Na_3SI are from ref 15.

revealed, then this knowledge might be exploited in the synthesis of Na_3SI and Li_3SI.

Here, *in situ* synchrotron X-ray diffraction is used to carefully map out the phase evolution during the formation of Ag_3SI as a function of temperature. Analogous experiments are performed on Na_3SI and Li_3SI as well. A comparison of reaction pathways for these three antiperovskites reveals that the formation of Ag_3SI occurs via a mechanism that is not accessible for Na_3SI and Li_3SI. In particular, the adoption of a common body centered cubic (bcc) packing of anions (S^{2-} or I^-) in the reactants at elevated temperatures facilitates the formation of the antiperovskite structure with the same bcc anion packing. *In situ* X-ray diffraction data, as shown in Figure 2a, reveal a series of phase evolutions during the heating of the 1:1 ratio mixture of AgI and Ag_2S, which are vacuum sealed in a quartz tube, from room temperature up to 600 °C. The annealing profile was chosen based on previous syntheses.[17,18]

The synthesis process can be categorized into three stages (Figure 2b−d). At room temperature, AgI crystallizes in the β-polymorph. This polymorph adopts space group $P6_3mc$, with hexagonal close packing (hcp) of I^-. Ag_2S crystallizes in the α-polymorph with space group $P2_1/c$, which has a distorted body centered cubic (bcc) packing of S^{2-}.[23,24] In the first stage, shown in Figure 2b, AgI and Ag_2S undergo phase transitions at ∼175 °C and ∼200 °C into α-AgI (*S.G. Im-3m*) and β-Ag_2S (*S.G. Im-3m*) respectively.[9,25] The polymorphs of the two binaries possess the same body centered cubic (bcc) packing of anions (I^-, S^{2-}), which also is the anion packing sequence for Ag_3SI antiperovskites (Figure 2e, Stage 1). Following these phase transitions, the diffraction peaks of α-AgI and β-Ag_2S shift to lower angles for temperatures up to 475 °C, as shown in Figure 2c. The linear correlations of the binaries' lattice parameters with temperature in this regime are consistent with thermal expansion (Figure S4).

In the second stage, corresponding to temperatures from 475 to 600 °C, broad Bragg peaks grow between the two binaries, indicating a continuous merging into an $Ag_xS_yI_{2-y}$ ($2 \leq x \leq 4$, $0 \leq y \leq 2$) solid-solution, which possesses the same bcc anion packing. After holding at 600 °C for 2.5 h, a set of symmetric diffraction peaks, indexed with $Im\bar{3}m$ symmetry, is observed. Further changes in peak positions and shapes are negligible, indicating that the distribution of S^{2-} and I^- in the $Ag_xS_yI_{2-y}$ solid solution has become homogeneous. Therefore, at the end of stage 2, an Ag_3SI phase with a random distribution of I^- and S^{2-} is formed.

Finally, in the subsequent cooling process (stage 3), the Ag_3SI phase maintains $Im\bar{3}m$ symmetry until the temperature reaches 210 °C. Another cubic phase with an extra *hkl* peak at 2.36 degrees starts to evolve as shown in Figure 2d. This new cubic phase can be indexed with a lower symmetry (Pm-$3m$), which has an extra ordering along the [111] direction. This extra ordering results from the rearrangement of S^{2-} and I^-. As shown in Figure 2e, stage 3, the center of the cubic lattice (0.5, 0.5, 0.5) is occupied by I^-, while the corners (0, 0, 0) are occupied by S^{2-}. Thus, the S/I ordered β-Ag_3SI is gradually transformed from the S/I disordered α-Ag_3SI at 200 °C. Nonetheless, after holding at 200 °C for 2 h, the α to β phase transition is still not complete. Upon lowering the temperature to 90 °C, new sharp diffraction peaks appeared at 2.85, 3.29,

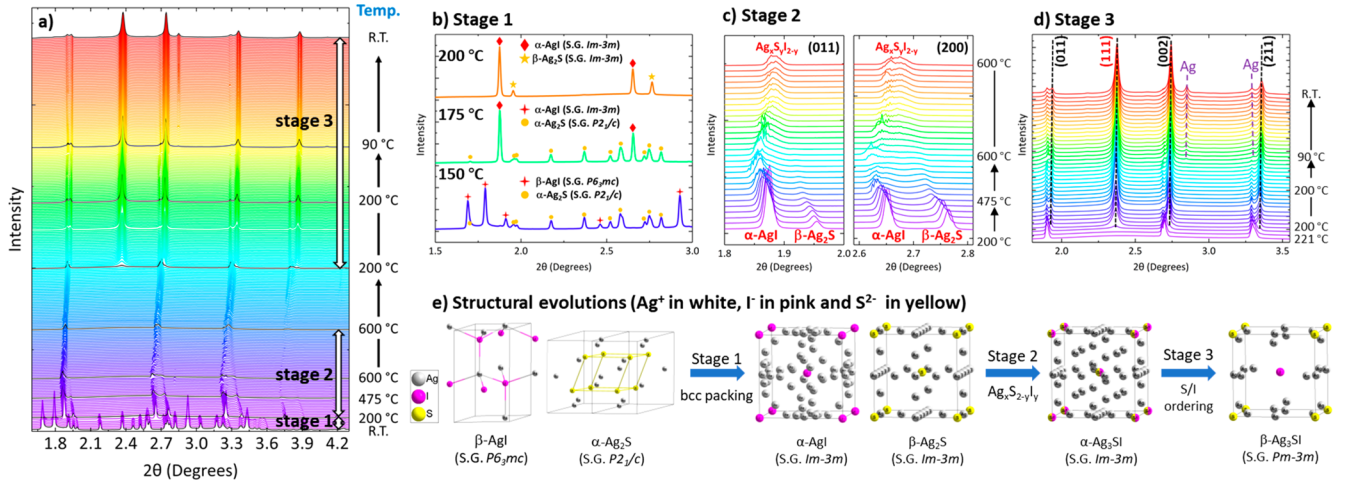

Figure 2. *In situ* synchrotron X-ray diffraction (sXRD) data collected during the synthesis of Ag_3SI with temperatures on the right side (a) and selected sXRD data for three major stages (b−d) with the representation of structural evolutions in each stage below (e).

https://dx.doi.org/10.1021/acs.inorgchem.0c01705
Inorg. Chem. 2020, 59, 11244−11247

and 4.65 degrees, which correspond to the diffraction peaks of Ag metal. The metallic silver may be the reduction product of excess Ag^+ by carbon, which is coated on the inner wall of quartz tube. Excess Ag^+ could originate from the evaporation of I at high temperatures. Filling the quartz tube with inert gas instead of vacuum sealing is expected to reduce Ag metal formation.

The final products obtained at room temperature consist of dominating β-Ag_3SI, minor α^*-Ag_3SI, and other byproducts, including Ag metal and the two binary reactants (Figure S5). It has been reported that α-Ag_3SI could dissociate itself into the binaries[18] or transform to α^*-Ag_3SI[10] during cooling. The instability of α-Ag_3SI compared with other polymorphs at low temperature agrees with the computed Gibbs free energies shown in Figure S2. In particular, the free energy of α-Ag_3SI is predicted to be larger than that of β-Ag_3SI below 314 K. Similarly, the formation energy of α-Ag_3SI relative to AgI and Ag_2S is predicted to become increasingly positive at low temperatures. (Figure 1)

On the basis of above *in situ* diffraction studies, the key step to form the Ag_3SI antiperovskite phase is the phase transformations of AgI and Ag_2S binaries into polymorphs having bcc anion packing. This facilitates the formation of the $Ag_xS_yI_{2-y}$ solid solution, which has a similar anion packing. The α–β phase transition around 200 °C is an important step to obtain the S^{2-}/I^- ordered β-Ag_3SI structure at room temperature. The minimum temperature for these two steps is approximately 200 °C, which is much lower than the common synthesis temperature for Ag_3SI. Moreover, the present DFT calculations shown in Figure S1 predict that α-Ag_3SI becomes stable at ∼80 °C relative to the AgI and Ag_2S reactants. In addition, since the ramping rate for the *in situ* synthesis was relatively fast, the high onset temperature observed for the merging process in stage 2 may be an artifact of the heating rate. To test this hypothesis, *ex situ* synthesis is attempted at 220 °C. As a comparison, another synthesis is conducted at 550 °C followed by holding at 220 °C. High-resolution X-ray diffraction data of the two products are shown in Figure S6. Rietveld refinements confirm that pure β-Ag_3SI can be obtained after holding the reaction temperature at 550 °C for 2 days followed by another 2 days at 220 °C. Interestingly, 70 wt % of β-Ag_3SI is obtained after annealing at 220 °C for 4 days. Lattice parameters of two β-Ag_3SI samples are almost identical: 4.9009 (4) Å versus 4.9031(1) Å. Therefore, the merging of bcc anion packing binaries can occur at a much lower temperature than that observed in the *in situ* measurement (475 °C).

In situ experiments are conducted to investigate the possible formation of Na_3SI and Li_3SI. As shown in Figure 3, both reactants, NaI and Na_2S, retain face centered cubic packing up to 650 °C. The Rietveld fit confirms two cubic binaries at 650 °C (Figure S7). Furthermore, their lattice parameters exhibit linear correlations with temperature, indicating that only thermal expansion has occurred. *In situ* studies on the synthesis of Li_3SI show the same result (Figure S8). Phase transitions to bcc anion packing of the initial binaries does not occur in the case of sodium and lithium compounds. The reason could be the low stability of the bcc anion packing of S^{2-} and I^- with occupations of Na^+ or Li^+ among the interspaces. According to previous literature,[25] in contrast to sodium and lithium iodides and sulfides, the bcc anion packing could be stabilized by the orbital mixing between Ag^+ (d orbitals) and I^-, S^{2-} (p orbitals) in silver analogues. Further

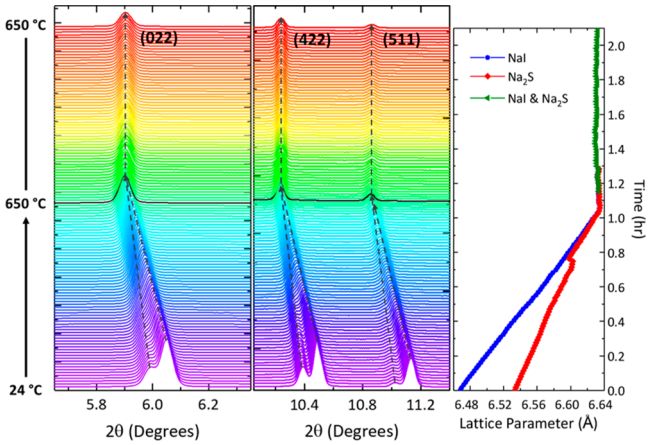

Figure 3. *In situ* sXRD data for the annealing of Na_2S/NaI mixture with temperature program labeled on the left. Changes in lattice parameters were plotted on the right.

increasing the synthesis temperature could be a strategy to bypass these barriers. However, any such strategy must address the consequences of evaporation of NaI and LiI, which was found to be severe very shortly after melting, as proved by the rapid mass loss measured in TGA/DSC measurements shown in Figure S9. We found that these vapors were extremely reactive against the quartz container used in these syntheses, even when coated with carbon, precluding any reaction between the two alkali metal binaries.

In conclusion, the stability and formation mechanism of Ag_3SI antiperovskite is investigated using *in situ* synchrotron X-ray diffraction and first-principles calculations. Three major stages are involved in the formation of the final S^{2-}/I^- ordered Ag_3SI polymorph. The formation of Ag_3SI is facilitated by phase transitions of the two reactants, Ag_2S and AgI, to structures having the same bcc anion packing. The merging of these two anion bcc packing binaries into Ag_3SI antiperovskite can initiate at as low as 220 °C. However, in the case of Na_2SI and Li_3SI, the adoption of a common bcc anion packing in the binary reactants does not occur below their melting points. This hinders the facile formation of the respective ternary antiperovskites.

■ ASSOCIATED CONTENT

Supporting Information

The Supporting Information is available free of charge at https://pubs.acs.org/doi/10.1021/acs.inorgchem.0c01705.

Experimental details of *in situ* and *ex situ* syntheses, computational methods, additional diffraction data for phase identification and Rietveld fits, *in situ* diffraction data for the synthesis of Li_3SI, TGA, and DSC data, details of additional figures and tables (PDF)

Rietveld fits of synchrotron data of *ex situ* synthesized Ag_3SI (condition 1) (TXT)

Rietveld fits of synchrotron data of *ex situ* synthesized Ag_3SI (condition 2) (TXT)

■ AUTHOR INFORMATION

Corresponding Author

Saul H. Lapidus − *X-ray Science Division, Advanced Photon Source, Argonne National Laboratory, Lemont, Illinois 60439, United States*; Email: slapidus@anl.gov

https://dx.doi.org/10.1021/acs.inorgchem.0c01705
Inorg. Chem. 2020, 59, 11244−11247

Authors

Liang Yin − *X-ray Science Division, Advanced Photon Source, Argonne National Laboratory, Lemont, Illinois 60439, United States*

Megan Murphy − *Department of Chemistry, University of Illinois at Chicago, Chicago, Illinois 60607, United States*

Kwangnam Kim − *Mechanical Engineering Department, University of Michigan, Ann Arbor, Michigan 48109-2125, United States;* orcid.org/0000-0003-1149-1733

Linhua Hu − *Department of Chemistry, University of Illinois at Chicago, Chicago, Illinois 60607, United States;* orcid.org/0000-0002-0177-3983

Jordi Cabana − *Department of Chemistry, University of Illinois at Chicago, Chicago, Illinois 60607, United States;* orcid.org/0000-0002-2353-5986

Donald J. Siegel − *Mechanical Engineering Department, University of Michigan, Ann Arbor, Michigan 48109-2125, United States;* orcid.org/0000-0001-7913-2513

Complete contact information is available at: https://pubs.acs.org/10.1021/acs.inorgchem.0c01705

Notes

The authors declare no competing financial interest.

■ ACKNOWLEDGMENTS

This work is supported by the Joint Center for Energy Storage Research (JCESR) of the U.S. Department of Energy (DOE). Use of the Advanced Photon Source at Argonne National Laboratory was supported by the U.S. Department of Energy, Office of Science, Office of Basic Energy Sciences, under Contract No. DE-AC02-06CH11357.

■ REFERENCES

(1) Zhang, Z.; Shao, Y.; Lotsch, B.; Hu, Y.-S.; Li, H.; Janek, J.; Nazar, L. F.; Nan, C.-W.; Maier, J.; Armand, M.; Chen, L. New horizons for inorganic solid state ion conductors. *Energy Environ. Sci.* **2018**, *11* (8), 1945−1976.

(2) Famprikis, T.; Canepa, P.; Dawson, J. A.; Islam, M. S.; Masquelier, C. Fundamentals of inorganic solid-state electrolytes for batteries. *Nat. Mater.* **2019**, *18* (12), 1278−1291.

(3) Janek, J.; Zeier, W. G. A solid future for battery development. *Nat. Energy* **2016**, *1* (9), 1−4.

(4) Zhao, C.; Liu, L.; Qi, X.; Lu, Y.; Wu, F.; Zhao, J.; Yu, Y.; Hu, Y.-S.; Chen, L. Solid-State Sodium Batteries. *Adv. Energy Mater.* **2018**, *8* (17), 1703012.

(5) Lim, H.-D.; Park, J.-H.; Shin, H.-J.; Jeong, J.; Kim, J. T.; Nam, K.-W.; Jung, H.-G.; Chung, K. Y. A review of challenges and issues concerning interfaces for all-solid-state batteries. *Energy Storage Mater.* **2020**, *25*, 224−250.

(6) Zhou, W.; Li, Y.; Xin, S.; Goodenough, J. B. Rechargeable Sodium All-Solid-State Battery. *ACS Cent. Sci.* **2017**, *3* (1), 52−57.

(7) Gao, Z.; Sun, H.; Fu, L.; Ye, F.; Zhang, Y.; Luo, W.; Huang, Y. Promises, Challenges, and Recent Progress of Inorganic Solid-State Electrolytes for All-Solid-State Lithium Batteries. *Adv. Mater.* **2018**, *30* (17), No. e1705702.

(8) Nanda, J.; Wang, C.; Liu, P. Frontiers of solid-state batteries. *MRS Bull.* **2018**, *43* (10), 740−745.

(9) Takahashi, T. Solid silver ion conductors. *J. Appl. Electrochem.* **1973**, *3* (2), 79−90.

(10) Hull, S.; Keen, D.; Madden, P.; Wilson, M. Ionic Diffusion within the α^* and β Phases of Ag_3SI. *J. Phys.: Condens. Matter* **2007**, *19* (40), 406214.

(11) Zhao, Y.; Daemen, L. L. Superionic conductivity in lithium-rich anti-perovskites. *J. Am. Chem. Soc.* **2012**, *134* (36), 15042−7.

(12) Wang, Y.; Wang, Q.; Liu, Z.; Zhou, Z.; Li, S.; Zhu, J.; Zou, R.; Wang, Y.; Lin, J.; Zhao, Y. Structural manipulation approaches towards enhanced sodium ionic conductivity in Na-rich antiperovskites. *J. Power Sources* **2015**, *293*, 735−740.

(13) Zhu, J.; Wang, Y.; Li, S.; Howard, J. W.; Neuefeind, J.; Ren, Y.; Wang, H.; Liang, C.; Yang, W.; Zou, R.; Jin, C.; Zhao, Y. Sodium Ion Transport Mechanisms in Antiperovskite Electrolytes Na_3OBr and Na_4OI_2: An in Situ Neutron Diffraction Study. *Inorg. Chem.* **2016**, *55* (12), 5993−8.

(14) Kim, K.; Siegel, D. J. Correlating lattice distortions, ion migration barriers, and stability in solid electrolytes. *J. Mater. Chem. A* **2019**, *7* (7), 3216−3227.

(15) Kim, K. *Computational Discovery of Solid Electrolytes for Batteries: Interfacial Phenomena and Ion Mobility*. PhD Thesis, University of Michigan, Ann Arbor, 2020.

(16) Emly, A.; Kioupakis, E.; Van der Ven, A. Phase stability and transport mechanisms in antiperovskite Li_3OCl and Li_3OBr superionic conductors. *Chem. Mater.* **2013**, *25* (23), 4663−4670.

(17) Takahashi, T.; Yamamoto, O. The $Ag/Ag_3SI/I_2$ solid-electrolyte cell. *Electrochim. Acta* **1966**, *11* (7), 779−789.

(18) Hoshino, S.; Sakuma, T.; Fujii, Y. A Structural Phase Transition in Superionic Conductor Ag_3SI. *J. Phys. Soc. Jpn.* **1979**, *47* (4), 1252−1259.

(19) Hull, S.; Keen, D.; Gardner, N.; Hayes, W. The crystal structures of superionic Ag_3SI. *J. Phys.: Condens. Matter* **2001**, *13* (10), 2295.

(20) Yan, S.; Xiao, H.; Liu, X. Rapid Fabrication and Thermal Performance of Ag_3SI Super-Ionic Conductor. *Chalcogenide Lett.* **2016**, *13* (10), 483−487.

(21) Didisheim, J.; McMullan, R.; Wuensch, B. A single-crystal neutron diffraction study of the distribution and thermal motion of silver ions in alpha- and beta- Ag_3SI. *Solid State Ionics* **1986**, *18*−*19*, 1150−1162.

(22) Chiodelli, G.; Magistris, A.; Schiraldi, A. Ag_3SBr and Ag_3SI: Ionic Conductivity of Their Modifications in the T Range 93−573 K. *Z. Phys. Chem. (Muenchen, Ger.)* **1979**, *118* (2), 177−186.

(23) Burley, G. Polymorphism of silver iodide. *Am. Mineral.* **1963**, *48* (11−12), 1266−1276.

(24) Sharma, R.; Chang, Y. The Ag-S (Silver-Sulfur) system. *Bull. Alloy Phase Diagrams* **1986**, *7* (3), 263−269.

(25) Wuensch, B. J. Silver and Copper Fast-Ion Conductors with Simple Anion Packings: Cation Distributions, Bonding, and Transport Behavior. *Solid State Ion.* **1992**, 291−313.